



Enhancement of oxygen sensing performance of metalloporphyrin film modified with nano Al₂O₃ powder

Honglin Zhang^{a,*}, Ke Zhang^b, Zhiguo Zhiguo^c, Jian Hao^d

^a College of General Education, Guangzhou Huali College, Guangzhou, 511325, China

^b MIIT Key Laboratory of Critical Materials Technology for New Energy Conversion and Storage, School of Chemistry and Chemical Engineering, Harbin Institute of Technology, Harbin, 150001, China

^c School of Instrumentation Science and Engineering, Harbin Institute of Technology, Harbin, 150001, China

^d State Key Laboratory of High-efficiency Utilization of Coal and Green Chemical Engineering, Ningxia University, Yinchuan, 750021, China

ARTICLE INFO

Keywords:

Oxygen sensing
Al₂O₃ modification
Stern-volmer equation

ABSTRACT

In this work, the metalloporphyrin film of PtOEP/Poly (St-co-TFEMA) modified by nano Al₂O₃ powder was prepared, and the enhancement performance of oxygen sensing was studied in detail. It was verified that the modified film extended the residence time of oxygen through the characterization of SEM. The phosphorescence intensity changes with the content of Al₂O₃ and PtOEP were studied. The Stern-Volmer equations before and after modification of Al₂O₃ powder was compared. It was found that the linearity of the calibration curve was still high, but the oxygen sensitivity value of K_{SV} was significantly improved due to the increase of quenching probability between indicator and oxygen. Finally, the stability test shows that the Al₂O₃@PtOEP/Poly (St-co-TFEMA) oxygen sensing film presents a strong anti-photo-bleaching ability, and the response time is shortened.

1. Introduction

Oxygen is not only an important component of respiration, but also provides energy for cell metabolism, supports combustion [1, 2]. Hyperbaric oxygen is an effective substance for the treatment of periodontal disease [3–5]. The content of dissolved oxygen in water is an important indicator to evaluate the deterioration of water quality [6–8]. In meteorological measurement, the pressure distribution of each measuring point at the same height can be calculated by measuring the oxygen partial pressure [9,10], which provides a basis for weather forecast. With the progress of science and technology, the standard of oxygen detection has also been improved. Therefore, the realization of accurate detection of oxygen content is of great significance to many fields of our production and life.

The optical oxygen measurement method based on room temperature phosphorescence (RTP) oxygen quenching principle [11,12] has the advantages of long luminescence lifetime, large Stokes shift [13–15], reversibility and anti-electromagnetic interference [16, 17]. In recent years, it has gradually replaced the traditional iodometric titration [18] and Clark electrode method [19], and has been widely used in the fields of clinical medicine, food safety, environmental detection and aquaculture. The existing oxygen sensing materials can meet some application requirements, but the low detection sensitivity limits the further development of the materials. It is expected to be an effective method to enhance the sensitivity by modifying the oxygen sensing materials to improve the oxygen

* Corresponding author.

E-mail address: zpp13125@163.com (H. Zhang).

<https://doi.org/10.1016/j.heliyon.2023.e18300>

Received 6 March 2023; Received in revised form 12 July 2023; Accepted 13 July 2023

Available online 17 July 2023

2405-8440/© 2023 The Author(s). Published by Elsevier Ltd. This is an open access article under the CC BY-NC-ND license (<http://creativecommons.org/licenses/by-nc-nd/4.0/>).

quenching sites. Nano alumina Al_2O_3 has the advantages of high chemical stability, strong adsorption capacity, large surface area, concentrated pore distribution and many surface active centers [20,21]. It has shown good affinity with various substrates, which can improve the compactness, corrosion resistance, smoothness and storage stability of materials, and gradually become an indispensable functional and structural material to promote social development. In addition, Nano Al_2O_3 can absorb ultraviolet light and emit the wavelength equivalent to the particle size under specific excitation, which can greatly improve the luminescence intensity [22].

In view of the merits of nano Al_2O_3 , scientists have carried out extensive research. Yousefi et al. [23] studied the effect of nano alumina filler on the mechanical properties of polymer-derived SiC coating firstly, found that 20% of nano alumina can activate the nucleation of SiC fiber and effectively improve the mechanical properties of the coating. Pitawala et al. [20] explored the influence of nano porous Al_2O_3 on the thermoelectric transport performance of polymer electrolyte. The structural modification of polymer caused by Al_2O_3 enhances the ionic conductivity, thus significantly improving the conductivity ($6.05 \times 10^{-5} \text{ S cm}^{-1}$). Zhou et al. [24] designed a Zn–Al LDH film based on nano porous anodic aluminum oxide. The photoluminescence (PL) intensity and surface enhanced fluorescence (SEF) factor of the films were increased by 2 and 6 times, respectively. It was revealed that the enhancement mechanism was attributed to the oxygen vacancy, and the larger surface area of 3D sheet structure could capture more fluorescent molecules. Zheng et al. [22] investigated the effect of thickness on the oxygen sensing properties of TiO_2 thin films on Al_2O_3 substrates. The optimal thickness is $2.3 \mu\text{m}$ by comparing the oxygen sensitivity and the response time varies with temperature.

In this study, the highly oxygen-sensitive PtOEP was chosen as the luminescence indicator. Meanwhile, PtOEP has the advantages of large Stokes shift, strong phosphorescent emission and well stability compared with other metalloporphyrins, which can effectively eliminate the interference of external environment on the test process. We aim to modify the fluoropolymer of Poly (St-co-TFEMA) with nano Al_2O_3 powder to enhance the interaction probability between indicator and oxygen molecule, and then improve the oxygen sensitivity. The oxygen sensitivity enhancement mechanism of nano Al_2O_3 was revealed by comparing the luminescence intensity Stern-Volmer calibration equations before and after modification, combined with the morphological characteristics. Furthermore, the effect of Al_2O_3 on photostability and repeatability were investigated.

2. Experimental section

2.1. Materials

Platinum octaethylporphine (PtOEP), Styrene (St) and trifluoroethyl methacrylate (TFEMA) were obtained from J&K Chemical Co., Ltd. Solvent of Xylene was from Xilong Chemical Reagent Co., Ltd. Nano $\alpha\text{-Al}_2\text{O}_3$ powder was purchased from Beijing Deke Daojin Science And Technology Co., Ltd, and 2, 2-Azobisisobutyronitrile (AIBN) was from Aladdin Chemical Co., Ltd. High-purity (99.99%) nitrogen and oxygen were from Harbin Liming Co., Ltd.

2.2. Preparation of Al_2O_3 @PtOEP/Poly (St-co-TFEMA) oxygen sensing film

The reaction monomers of St and TFEMA were extracted and washed repeatedly with 1 wt% NaOH solution and ultrapure water to remove the polymerization inhibitor of hydroquinone, then stored at low temperature after dried with anhydrous MgSO_4 . In addition, the initiator AIBN needs to be recrystallized to achieve purification. The co-polymer of Poly (St-co-TFEMA) was prepared by solvothermal method. Firstly, 0.0090 g/mL AIBN/xylene was uniformly disperse in 15 mL mixed solution of St/xylene and TFEMA/xylene (concentration ratio of 1:1) to realize premixing. The mixture were added into the three-necked flask with a reflux condenser and nitrogen inlet. The copolymerization reaction was takes place for 7 h under the condition of 72°C and stirring speed was 300 rpm. Co-polymers were reprecipitated with methanol to remove unreacted monomers. Then the film preparation process was shown in Fig. 1. The co-polymer solution were uniformly mixed with the PtOEP/xylene (1 mM) and Al_2O_3 /xylene solution (2 mM). The thickness was controlled by a film applicator with controllable thickness of $30 \mu\text{m}$. Then the Al_2O_3 @PtOEP/Poly (St-co-TFEMA) oxygen sensing film were obtained by coating the mixed solution onto quartz glass (size specification: $45 \times 12 \times 1 \text{ mm}$) after dried for

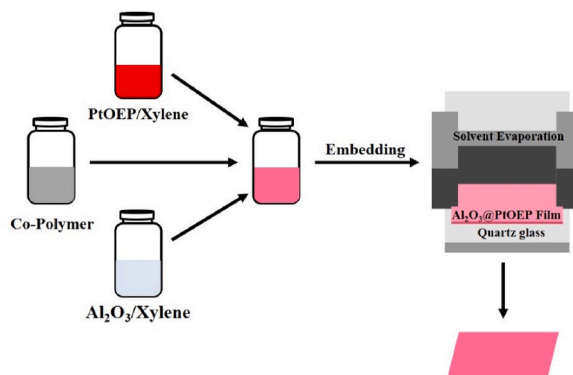


Fig. 1. Schematic diagram of preparation of Al_2O_3 powder modified metalloporphyrin oxygen sensing film.

8 h and stored in the dark place.

2.3. Instruments and characterization

During the test process, the surface and sectional morphology of $\text{Al}_2\text{O}_3@\text{PtOEP}/\text{Poly}(\text{St-co-TFEMA})$ sensing film was characterized by scanning electron microscope (SEM, SUPRA 55 SAPPHIRE). The properties of the copolymer were characterized by infrared spectrum (IR, Nicolet is5003190721) and mass spectrometry (MS, STA449F3-QMS403D-Is 50). The oxygen sensing performance test device were shown in Fig. 2, which are composed of the following parts: a laser lamp with central wavelength at 405 nm was chosen as excitation light source (continuous wave with excitation light power of $0.2 \text{ mW}/\text{cm}^2$), the miniaturized optical spectrometer (USB2000) was used as the signal detector to record luminescence spectrum. Simultaneous acquisition of phosphorescent excitation and detection signals by coupled fiber. A nitrogen/oxygen mixing equipment (pure nitrogen, pure oxygen, nitrogen/oxygen mixing chamber) were used to adjust oxygen partial pressure under the total gas mixture pressure of 100 kPa and the ambient temperature of $25 \text{ }^\circ\text{C}$.

3. Results and discussion

3.1. SEM characterization of PtOEP/Poly (St-co-TFEMA) film without and with Al_2O_3 powder

Fig. S2 shows the properties of the Poly (St-co-TFEMA) obtained from the IR and MS characterization, which results verified the successful synthesized of copolymer with the molecular weight of 168000. In the preparation process of PtOEP/Poly (St-co-TFEMA) oxygen sensing film, although a film coating device was chosen to control the thickness. However, a large amount of toluene solvent evaporates during the film drying process, so the actual film thickness needs to be given in conjunction with SEM results. The surface and sectional morphology of PtOEP/Poly (St-co-TFEMA) sensing film without and with Al_2O_3 powder were shown in Fig. 3a, Fig. 3c and b, Fig. 3d, respectively. The surface morphology of PtOEP/Poly (St-co-TFEMA) film presents a heterogeneous porous structure with the pore size of the film are $10.5 \pm 0.4 \text{ }\mu\text{m}$ and $8.8 \pm 0.3 \text{ }\mu\text{m}$. In comparison, the $\text{Al}_2\text{O}_3@\text{PtOEP}/\text{Poly}(\text{St-co-TFEMA})$ sensing film has a smooth and uniform porous surface structure with a size of $1.0 \pm 0.1 \text{ }\mu\text{m}$, and the gaussian distribution plot of measured pore size were shown in Fig. S1. The cross-sectional SEM characterization results show that the thickness of the two films were $14.4 \pm 0.2 \text{ }\mu\text{m}$ and $15.8 \pm 0.3 \text{ }\mu\text{m}$, respectively. The SEM results indicate that the doping of Al_2O_3 powder has little effect on the thickness, but it reduces the pore size of the film and forms a denser internal structure, which will greatly enhance the stability of the film and prolong the residence time of oxygen inside the film, increase the value of oxygen sensitivity. Meanwhile, the structure with uniform pore size can effectively ensure the uniform distribution of sensitivity in the film, thus enhancing the linearity of the oxygen content calibration equation.

3.2. Variation of phosphorescence intensity changes with $\text{Al}_2\text{O}_3/\text{xylenes}$ concentration and PtOEP/xylenes

Since the fluoropolymer is a non-luminescent material (Fig. S3), the phosphorescence intensity of the film are only related to the amount of $\text{Al}_2\text{O}_3/\text{xylenes}$ and PtOEP/xylenes. Fig. 4a and b explore the phosphorescence intensity of oxygen sensing film changes with $\text{Al}_2\text{O}_3/\text{xylenes}$ and PtOEP/xylenes concentration. The results show that the intensity increases first and then decreases with the

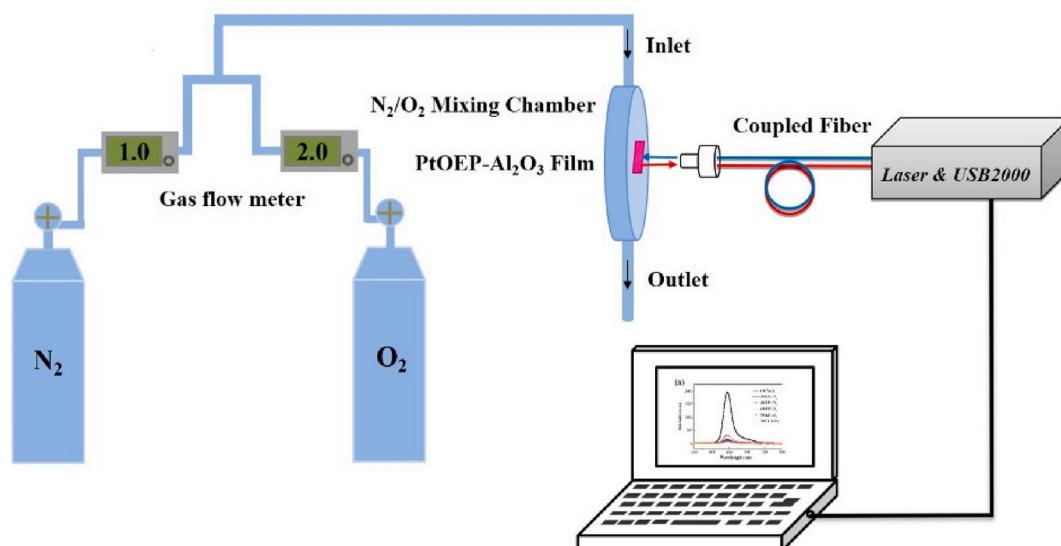


Fig. 2. The device for testing the luminescence spectrum of $\text{Al}_2\text{O}_3@\text{PtOEP}/\text{Poly}(\text{St-co-TFEMA})$ sensing film.

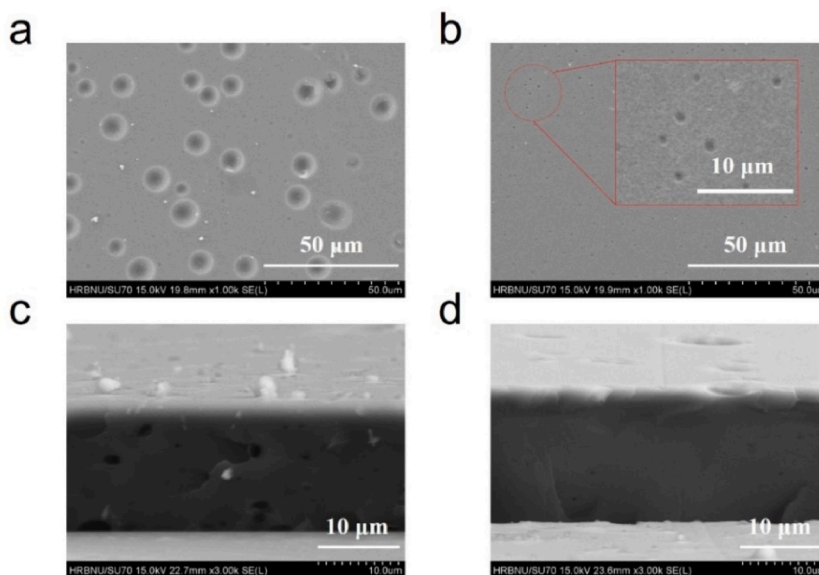


Fig. 3. Comparison of surface and sectional morphology between PtOEP/Poly (St-co-TFEMA) film oxygen sensing film: (a) (c) Without Al₂O₃ Powder; (b) (d) With Al₂O₃ Powder.

increase of Al₂O₃/xylenes concentration. It was indicated that the phosphorescence intensity can be improved with the appropriate amount of Al₂O₃ powder. However, adhesion phenomenon occurred among the Al₂O₃ powder when its amount exceeds 2 mM, which will change the propagation path of the light in the film, leading to the reduction of the intensity, and this will also directly affect the oxygen sensitivity. The relationship between the phosphorescence intensity and the PtOEP/xylenes concentration meets a similar tendency, which is due to the self-quenching phenomenon between indicators when the PtOEP concentration is excessive, resulting in the attenuation of the luminescence signal.

3.3. The Stern-Volmer equation of Al₂O₃@PtOEP/Poly (St-co-TFEMA) film

RTP oxygen sensing materials are based on dynamic quenching mechanism [11,25]. As a typical luminescent quenching agent, oxygen in the ground state will produce singlet oxygen after interacting with triple-excited state phosphors, which leads to the reduction of phosphorescent emission. The Stern-Volmer equation [12] is used to describe the quantitative relationship between the dynamic quenching degree of RTP and oxygen content, which expression is shown in equation 1-1.

$$\frac{I_{p0}}{I_p} = 1 + K_{SV}[O_2] \quad (1-1)$$

The slope of K_{SV} in the formula is the oxygen sensitivity, I_{p0} and I_p represent the phosphorescence intensity in the absence and

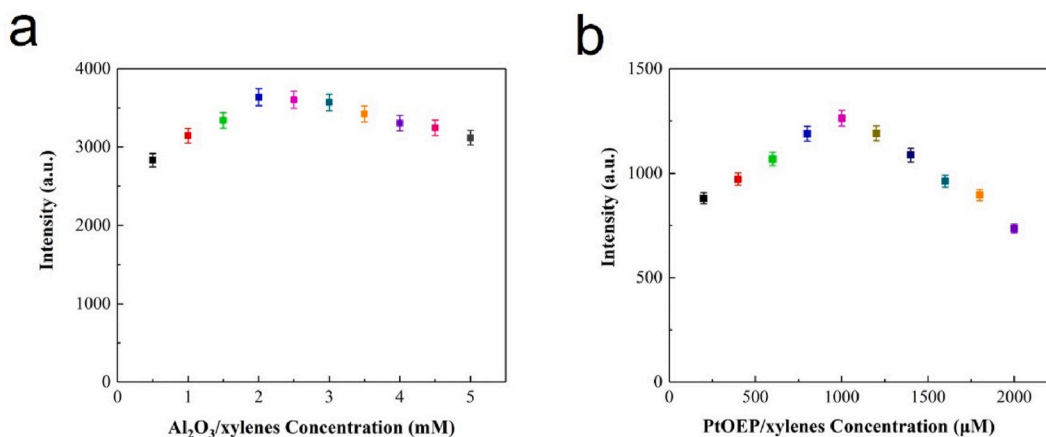


Fig. 4. The variation of phosphorescence intensity under different condition: (a) Al₂O₃/xylenes concentration; (b) PtOEP/xylenes concentration.

presence of oxygen and in the presence of oxygen, and I_{P0}/I_P is defined as the quenching ratio. Fig. 5a shows the phosphorescence intensity of $\text{Al}_2\text{O}_3@/\text{PtOEP}/\text{Poly}$ (St-co-TFEMA) oxygen sensing film under different oxygen partial pressures. It was found that the luminescence intensity of the sensing film decreased significantly with the increase of oxygen content, showing a strong phosphorescent quenching property. Furthermore, the comparison of Stern-Volmer equation of $\text{Al}_2\text{O}_3@/\text{PtOEP}$ film in contrast with unmodified PtOEP oxygen sensing film were obtained, which is shown in Fig. 5b. The results indicate that there is a high linear correlation between I_{P0}/I_P and the partial pressure of oxygen of $[\text{O}_2]$. It is calculated that K_{SV} value of PtOEP film before modification is 16.45 kPa^{-1} , while the K_{SV} value of modified $\text{Al}_2\text{O}_3@/\text{PtOEP}$ film was increased to 28.60 kPa^{-1} , which shows that the oxygen detection sensitivity has been significantly enhanced. Meanwhile, the K_{SV} value is significantly improved compared with pure PS film [26], and the calibration equation shows a higher linearity, as well as our previous study of PtOEP/Poly (p-SFt-co-TFEMA) oxygen sensing film [27]. In addition, the Stern-Volmer equation in gas and liquid environments were also compared in Fig. S4. The enhanced oxygen sensitivity is mainly attributed to the presence of Al_2O_3 powder prolong the diffusion path of oxygen molecules in the film, increasing the dynamic quenching sites between the indicator PtOEP and oxygen. After multiple movements of oxygen molecules, the quenching effect of oxygen on the indicator is more sufficient, thereby increasing the probability of interaction between the indicator and oxygen molecules, which directly reflecting on the improvement of oxygen sensitivity values. Moreover, the doping of Al_2O_3 powder enhances the mechanical stability of the oxygen sensing film and plays a more effective role in protecting indicator. Therefore, the interaction probability between oxygen and indicator is also improved.

3.4. The optical stability and repeatability of $\text{Al}_2\text{O}_3@/\text{PtOEP}/\text{Poly}$ (St-co-TFEMA) film

Under the condition of excitation light power of $0.6 \text{ mW}/\text{cm}^2$, Fig. 6a shows the normalized phosphorescence intensity of $\text{Al}_2\text{O}_3@/\text{PtOEP}/\text{Poly}$ (St-co-TFEMA) (solid-black-square) and PtOEP/Poly (St-co-TFEMA) (hollow-red-square) oxygen sensing film varies with time in pure N_2 saturated aqueous solution. It can be seen that the attenuation ratio of the oxygen sensing film is only 3.0% after continuous irradiation of 405 nm semiconductor laser for 2 h, which is lower than 4.5% of PtOEP/Poly (St-co-TFEMA) film. This indicate that the optical stability of the oxygen sensing film have been improved after modified by Al_2O_3 powder. Furthermore, Fig. 6b shows the normalized phosphorescence intensity attenuation of $\text{Al}_2\text{O}_3@/\text{PtOEP}$ film (solid-blue-circle) and PtOEP (hollow-pink-circle) film under 5.0 kPa O_2 saturated aqueous solution. The comparison results show that the photo-bleaching time in oxygenation environment is prolonged due to the stronger protection of $\text{Al}_2\text{O}_3@/\text{PtOEP}/\text{Poly}$ (St-co-TFEMA) film against PtOEP by doping of Al_2O_3 powder.

Fig. 7 measured the variation of normalized phosphorescence intensity of PtOEP film (red-solid) and $\text{Al}_2\text{O}_3@/\text{PtOEP}$ film (black-hollow) after alternate switching between pure nitrogen and pure oxygen saturated aqueous solution for 3 times (Fig. S5 was the comparison in gas and liquid environment). The quenching time t_Q of the two oxygen sensing films are 20 s and 10 s by calculating the time that the phosphorescence intensity decreased by 90%. The recovery time t_R are 250 s and 180 s, respectively. It was shown that the Al_2O_3 powder modified film has a faster response time, which is helpful to shorten the test time of the oxygen sensing film in practical applications. Phosphorescence signal attenuation phenomenon occurs in both $\text{Al}_2\text{O}_3@/\text{PtOEP}$ film and PtOEP film after 3 cycles of testing. Among them, the phosphorescence intensity retention rate of $\text{Al}_2\text{O}_3@/\text{PtOEP}$ film is 98.8%, which is significantly higher than 94.9% of PtOEP film, showing good repeatability.

4. Conclusion

In summary, the enhancement of oxygen sensing performance of fluoropolymer film modified with nano Al_2O_3 powder was investigated. SEM characterization shows that the doping of Al_2O_3 increases the density of film surface morphology. The variation of

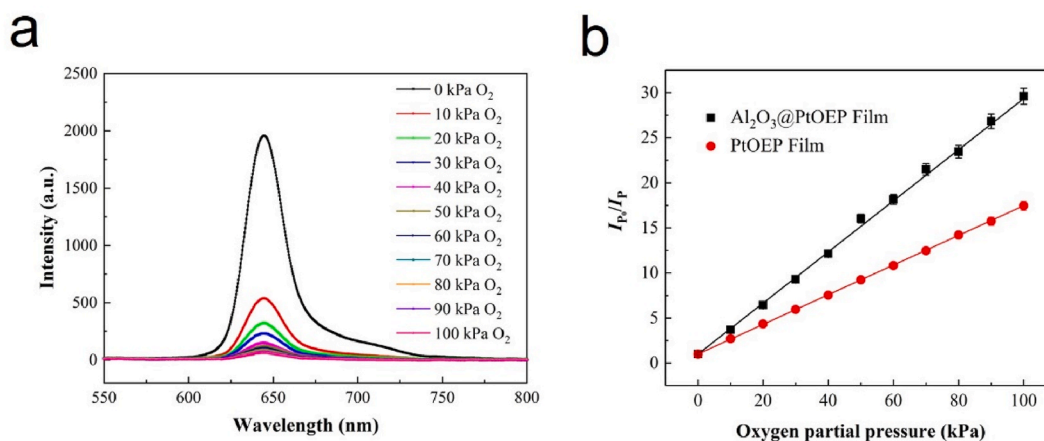


Fig. 5. The $\text{Al}_2\text{O}_3@/\text{PtOEP}/\text{Poly}$ (St-co-TFEMA) film: (a) Oxygen quenching curve; (b) Stern-Volmer equation.

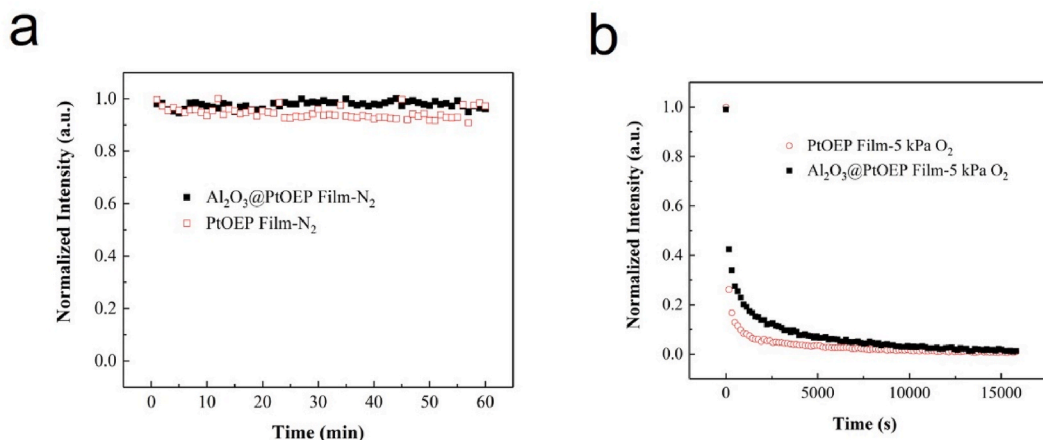


Fig. 6. The phosphorescence intensity of oxygen sensing film changes with time: (a) Al₂O₃@PtOEP (solid-black-square) and PtOEP (hollow-red-square) film in pure N₂ saturated aqueous solution; (b) Al₂O₃@PtOEP (solid-black-square) and PtOEP (hollow-red-square) film in 5.0 kPa O₂ saturated aqueous solution. (For interpretation of the references to colour in this figure legend, the reader is referred to the Web version of this article.)

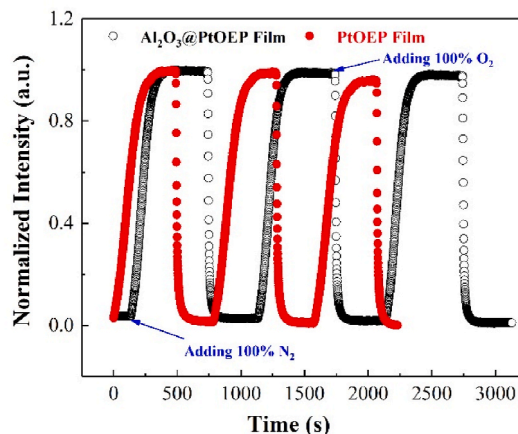


Fig. 7. The normalized repeatability between PtOEP film (red-solid) and Al₂O₃@PtOEP film (black-hollow). (For interpretation of the references to colour in this figure legend, the reader is referred to the Web version of this article.)

phosphorescence intensity change with Al₂O₃/xylenes and PtOEP/xylenes concentration were given. The Stern-Volmer equation of PtOEP oxygen sensing film before and after Al₂O₃ modification showed high linear correlation, but the K_{SV} value was increased from 16.45 kPa⁻¹ to 28.60 kPa⁻¹, which owing to the doping of Al₂O₃ powder enhanced the effective quenching site and improve the collision probability between the indicator and oxygen. In addition, the Al₂O₃@PtOEP/Poly (St-co-TFEMA) oxygen sensing film shows strong photo stability with the luminescence intensity attenuation ratio was 3.0%, and the response time of Al₂O₃@PtOEP film was calculated to be 10 s and 180 s, respectively. Consequently, a method to enhance the oxygen sensitivity by Al₂O₃ powder modified metalloporphyrin film was established to achieve accurate oxygen content detection.

Author contribution statement

Honglin Zhang: conceived and designed the experiments, performed the experiments, analyzed and interpreted the data, contributed reagents, materials, analysis tools or data, wrote the paper. Ke Zhang; Zhiguo Zhang; Jian Hao: contributed reagents, materials, analysis tools or data.

Funding statement

This work was supported by the Guangdong Provincial University Youth Innovative Talent Program (Grant No. 2022KQNCX163), and Foundation of State Key Laboratory of High-efficiency Utilization of Coal and Green Chemical Engineering (Grant No. 2022-K66).

Data availability statement

The data that has been used is confidential.

Declaration of competing interest

The authors declare that they have no known competing financial interests or personal relationships that could have appeared to influence the work reported in this paper.

Appendix A. Supplementary data

Supplementary data to this article can be found online at <https://doi.org/10.1016/j.heliyon.2023.e18300>.

References

- [1] F. Vincenzo, F. Belfiore, R. Maiolino, F. Matteucci, P. Ventura, Nitrogen and oxygen abundances in the local universe, *Mon. Not. Roy. Astron. Soc.* 458 (4) (2016) 3466–3477.
- [2] D.J. Gibbs, M.J. Holdsworth, Every breath you take: new insights into plant and animal oxygen sensing, *Cell* 180 (1) (2020) 22–24.
- [3] R. Maestri, E. Robbi, M. Lovagnini, C. Bruschi, M.T. La Rovere, G.D. Pinna, Arterial oxygen saturation during Cheyne-Stokes respiration in heart failure patients: does measurement site matter? *Sleep Med.* 55 (2019) 6–13.
- [4] W. Zhang, F. Ge, C. Lian, R. Xia, B. Zhang, A single-center observational clinical study on factors associated with regional cerebral oxygen saturation in full-term newborn infants during birth transition, *Med. Sci. Mon. Int. Med. J. Exp. Clin. Res.* 27 (2021), e928750.
- [5] R. Takegawa, K. Hayashida, D.M. Rolston, T. Li, S.J. Miyara, M. Ohnishi, T. Shiozaki, L.B. Becker, Near-infrared spectroscopy assessments of regional cerebral oxygen saturation for the prediction of clinical outcomes in patients with cardiac arrest: a review of clinical impact, evolution, and future directions, *Front. Med.* 7 (2020), 587930.
- [6] H. Tao, A.M. Bobaker, M.M. Ramal, Z.M. Yaseen, M.S. Hossain, S. Shahid, Determination of biochemical oxygen demand and dissolved oxygen for semi-arid river environment: application of soft computing models, *Environ. Sci. Pollut. Control Ser.* 26 (1) (2018) 923–937.
- [7] F. Villate, A. Iriarte, I. Uriarte, L. Intxausti, A. De La Sota, Dissolved oxygen in the rehabilitation phase of an estuary: influence of sewage pollution abatement and hydro-climatic factors, *Mar. Pollut. Bull.* 70 (1–2) (2013) 234–246.
- [8] E. Sánchez, M.F. Colmenarejo, J. Vicente, A. Rubio, M.G. García, L. Travieso, R. Borja, Use of the water quality index and dissolved oxygen deficit as simple indicators of watersheds pollution, *Ecol. Indic.* 7 (2) (2007) 315–328.
- [9] M. Akram, M.H. Akhtar, M. Irfan, Y. Tian, Polymer matrix: a good substrate material for oxygen probes used in pressure sensitive paints, *Adv. Colloid Interface Sci.* 283 (2020), 102240.
- [10] J.S. Kwak, Y.G. Choi, Oxygen sensitivity of photoluminescence intensity of Pt complex dispersed in fluorinated acrylate for pressure sensitive paint applications, *Electron. Mater.* 10 (5) (2014) 991–995.
- [11] E. Ciotta, P. Proposito, R. Pizzoferrato, Positive curvature in Stern-Volmer plot described by a generalized model for static quenching, *J. Lumin.* 206 (2019) 518–522.
- [12] M.H. Gehlen, The centenary of the Stern-Volmer equation of fluorescence quenching: from the single line plot to the SV quenching map, *J. Photochem. Photobiol. C Photochem. Rev.* 42 (2020), 100338.
- [13] S.H. Chao, M.R. Holl, S.C. McQuaide, T.T. Ren, S.A. Gales, D.R. Meldrum, Phosphorescence lifetime based oxygen microsensing using a digital micromirror device, *Opt Express* 15 (17) (2007) 10681–10689.
- [14] P.W. Zach, S.A. Freunberger, I. Klimant, S.M. Borisov, Electron-deficient near-infrared Pt(II) and Pd(II) benzoporphyrins with dual phosphorescence and unusually efficient thermally activated delayed fluorescence: first demonstration of simultaneous oxygen and temperature sensing with a single emitter, *ACS Appl. Mater. Interfaces* 9 (43) (2017) 38008–38023.
- [15] M. Eltermann, V. Kiisk, A. Berholts, L. Dolgov, S. Lange, K. Utt, R. Jaanisoo, Modeling of luminescence-based oxygen sensing by redox-switched energy transfer in nanocrystalline $\text{TiO}_2\text{:Sm}^{3+}$, *Sensor. Actuator. B Chem.* 265 (2018) 556–564.
- [16] C.J. Easley, M. Mettry, E.M. Moses, R.J. Hooley, C.J. Bardeen, Boosting the heavy atom effect by cavitand encapsulation: room temperature phosphorescence of pyrene in the presence of oxygen, *J. Phys. Chem.* 122 (32) (2018) 6578–6584.
- [17] Y. Xiong, J. Tan, C. Wang, Y. Zhu, S. Fang, J. Wu, Q. Wang, M. Duan, A miniaturized oxygen sensor integrated on fiber surface based on evanescent-wave induced fluorescence quenching, *J. Lumin.* 179 (2016) 581–587.
- [18] A. Carvalho, R. Costa, S. Neves, C.M. Oliveira, R.J.N. Bettencourt Da Silva, Determination of dissolved oxygen in water by the Winkler method: performance modelling and optimisation for environmental analysis, *Microchem. J.* 165 (2021), 106129.
- [19] F. Liebisch, A. Weltin, J. Marzloch, G.A. Urban, J. Kieninger, Zero-consumption Clark-type microsensor for oxygen monitoring in cell culture and organ-on-chip systems, *Sensor. Actuator. B Chem.* 322 (2020), 128652.
- [20] H.M.J.C. Pitawala, M.A.K.L. Dissanayake, V.A. Seneviratne, B.E. Mellander, I. Albinsson, Effect of nano-porous alumina filler on thermal and electrical transport properties of solid polymer electrolyte (PEO)₁₂LiBF₄, *Adv. Mater. Res.* 55–57 (2008) 745–748.
- [21] J. Exner, M. Schubert, D. Hanft, T. Stöcker, P. Fuierer, R. Moos, Tuning of the electrical conductivity of Sr(Ti,Fe)O₃ oxygen sensing films by aerosol co-deposition with Al₂O₃, *Sensor. Actuator. B Chem.* 230 (2016) 427–433.
- [22] L. Zheng, T. Xu, G. Li, Q. Yin, Influence of thickness on oxygen-sensing properties of TiO₂ thin films on Al₂O₃, *Jpn. J. Appl. Phys.* 41 (Part 1, No. 7A) (2002) 4655–4658.
- [23] M. Yousefi, M. Ghatee, M. Rezakazemi, S.H. Ghaderi, The effects of adding nano-alumina filler on the properties of polymer-derived SiC coating, *Int. J. Appl. Ceram. Technol.* 18 (6) (2021) 2197–2206.
- [24] Y. Zhou, X. Li, K. Wang, F. Hu, C. Zhai, X. Wang, J. Bai, Enhanced photoluminescence emission and surface fluorescence response of morphology controllable nano porous anodized alumina Zn-Al LDH film, *J. Alloys Compd.* 770 (2019) 6–16.
- [25] N. Shehata, K. Meehan, D.E. Leber, Fluorescence quenching in ceria nanoparticles: dissolved oxygen molecular probe with relatively temperature insensitive Stern-Volmer constant up to 50°C, *J. Nanophotonics* 6 (1) (2012), 063529.
- [26] D.H. Song, H.D. Kim, K.C. Kim, Dissolved oxygen concentration field measurement in micro-scale water flows using PtOEP/PS film sensor, *Opt Laser. Eng.* 50 (1) (2012) 74–81.
- [27] H.L. Zhang, T. Liu, M. Xu, F. Qin, Z.G. Zhang, Y. Tian, Oxygen-sensing properties of a highly sensitive and anti-photo-bleaching fluoropolymer film, *Mater. Lett.* 251 (2019) 165–168.